INTERNATIONAL JOURNAL FOR NUMERICAL AND ANALYTICAL METHODS IN GEOMECHANICS, VOL. 12, 61–77 (1988)

LOWER BOUND LIMIT ANALYSIS USING FINITE ELEMENTS AND LINEAR PROGRAMMING

S. W. SLOAN

Department of Civil Engineering and Surveying, The University of Newcastle, N.S.W., 2308, Australia

SUMMARY

This paper describes a technique for computing lower bound limit loads in soil mechanics under conditions of plane strain. In order to invoke the lower bound theorem of classical plasticity theory, a perfectly plastic soil model is assumed, which may be either purely cohesive or cohesive-frictional, together with an associated flow rule. Using a suitable linear approximation of the yield surface, the procedure computes a statically admissible stress field via finite elements and linear programming. The stress field is modelled using linear 3-noded triangles and statically admissible stress discontinuities may occur at the edges of each triangle. Imposition of the stress-boundary, equilibrium and yield conditions leads to an expression for the collapse load which is maximized subject to a set of linear constraints on the nodal stresses. Since all of the requirements for a statically admissible solution are satisfied exactly (except for small round-off errors in the optimization computations), the solution obtained is a strict lower bound on the true collapse load and is therefore 'safe'.

A major drawback of the technique, as first described by Lysmer,[1] is the large amount of computer time required to solve the linear programming problem. This paper shows that this limitation may be avoided by using an active set algorithm, rather than the traditional simplex or revised simplex strategies, to solve the resulting optimization problem. This is due to the nature of the constraint matrix, which is always very sparse and typically has many more rows than columns. It also proved that the procedure can, without modification, be used to derive strict lower bounds for a purely cohesive soil which has increasing strength with depth. This important class of problem is difficult to tackle using conventional methods. A number of examples are given to illustrate the effectiveness of the procedure.

INTRODUCTION

The lower bound theorem of classical plasticity theory is a powerful tool for analysing the stability of problems in soil mechanics. The theory assumes a perfectly plastic soil model with an associated flow rule and states that any statically admissible stress field will furnish a lower bound (or 'safe') estimate of the true limit load. A statically admissible stress field is one which satisfies (a) the stress boundary conditions, (b) equilibrium, and (c) the yield condition (the stresses must lie inside or on the yield surface in stress space).

Although the lower bound theorem is a particularly useful tool for the analysis of stability, it is often difficult to apply to practical problems involving complicated loading and complex geometry if it is necessary to construct the stress fields manually. Comprehensive discussions of the application of the lower bound theorem to geotechnical problems may be found in Davis[2] and Chen.[3] An alternative method of computing lower bounds, which uses finite elements and linear programming, has been presented by Lysmer.[1] In this procedure the soil mass is discretized into a collection of 3-noded triangular elements with the nodal variables being the unknown stresses. Statically admissible stress discontinuities are permitted to occur at the interfaces between adjacent triangles. Application of the stress-boundary conditions, equilibrium equations and yield criterion

0363–9061/88/010061–17$08.50

Received 27 January 1987

leads to an expression for the collapse load which is maximized subject to a set of linear constraints on the stresses. In order to avoid nonlinear constraints occurring in the constraint matrix, the yield criterion must be expressed as a linear function of the unknown stresses. For the Tresca and Mohr–Coulomb yield criteria, this is achieved by employing a polygonal approximation to the yield surface. The polygon is defined so that it lies inside the parent yield surface, thus ensuring that the solution obeys the conditions of the lower bound theorem. Other investigators who have studied the computation of lower bound limit loads by finite elements and linear programming include Anderheggen and Knopfel,[4] Pastor[5] and Bottero *et al.*[6] Optimal lower bounds for passive earth pressure problems, using finite elements and nonlinear programming, have been derived by Basudhar *et al.*[10] Another method of limit analysis, which employs a mixed finite element formulation and unconstrained minimization, has been proposed by Casciaro and Cascini.[11] This technique appears to give reasonably accurate estimates of collapse loads but the solutions are neither strict upper bounds nor strict lower bounds. Moreover, the stress and displacement fields may be subject to spurious oscillations.

A major advantage of the numerical formulation of the lower bound theorem is that complex loadings and geometries can be dealt with. Moreover, inhomogeneous soil properties can be modelled. Indeed, it will be shown in this paper that the technique can, without modification, be used to compute rigorous lower bounds on the limit load for purely cohesive soils which have strength increasing linearly with depth. This important class of problem is difficult to analyse using conventional procedures. The principal disadvantage of the technique is that significant amounts of computation time may be necessary to solve the resulting linear programming problem, especially if the traditional simplex or revised simplex algorithms are used. This is because the linearized yield criterion typically generates a very large number of inequality constraints on the nodal stresses. Lysmer[1] attempted to overcome this problem by employing an iterative technique which used a small subset of the total number of yield constraints. Although this approach reduces the computational effort significantly it may, in some cases, be unstable. This is because the method assumes that the path followed by each nodal stress during the optimization process will be relatively localized. If this is not the case, then the linear programming problem may become unbounded.

In this paper, an active set strategy is employed to solve the resulting linear programming problem. This algorithm, which has recently been published by Best and Ritter,[7] is shown to be ideally suited to the type of problem generated by the numerical implementation of the lower bound theorem. In particular, very large numbers of constraints on the nodal stresses may be imposed without a severe penalty on computational efficiency. Moreover, the canonical form required by the algorithm follows naturally from the numerical formulation of the lower bound theorem. To illustrate the effectiveness of the procedure, a number of footing problems are analysed and the results compared with known exact solutions (including one example of a purely cohesive soil which has strength increasing with depth).

THEORY

The formulation used in this paper follows that of Bottero *et al.*[6] Although the formulation proposed by Lysmer[1] requires a smaller number of variables, and hence is potentially more efficient, it often leads to a constraint matrix with terms of widely varying magnitude. This occurs, for example, if long thin elements are used or if a large number of segments are used to linearize the yield condition. In contrast, the formulation of Bottero *et al.*[6] generally results in a constraint matrix whose terms vary by only a few orders of magnitude. As can be expected, the conditioning of

the constraint matrix plays a critical role in the performance of linear programming algorithms. Although a number of heuristic schemes exist for scaling the constraint matrix automatically (see, for example, Reference 8), these have so far proved to be unreliable.

The triangular element used to model the stress field under conditions of plane strain is shown in Figure 1. The variation of the stress throughout each element is linear and each node is associated with 3 unknown stresses σ_x, σ_y and τ_{xy}. Each stress varies throughout an element according to

$$\sigma_x = \sum_{i=1}^{3} N_i \sigma_{xi}; \quad \sigma_y = \sum_{i=1}^{3} N_i \sigma_{yi}; \quad \tau_{xy} = \sum_{i=1}^{3} N_i \tau_{xyi} \tag{1}$$

where σ_{xi}, σ_{yi} and τ_{xyi} are the nodal stresses and N_i are linear shape functions. The latter are given by

$$N_1 = (\xi_1 + \eta_1 x + \zeta_1 y)/2A; \quad N_2 = (\xi_2 + \eta_2 x + \zeta_2 y)/2A; \quad N_3 = (\xi_3 + \eta_3 x + \zeta_3 y)/2A \tag{2}$$

where

$$\begin{aligned} \xi_1 &= x_2 y_3 - x_3 y_2; \quad & \eta_1 &= y_2 - y_3; \quad & \zeta_1 &= x_3 - x_2 \\ \xi_2 &= x_3 y_1 - x_1 y_3; \quad & \eta_2 &= y_3 - y_1; \quad & \zeta_2 &= x_1 - x_3 \\ \xi_3 &= x_1 y_2 - x_2 y_1; \quad & \eta_3 &= y_1 - y_2; \quad & \zeta_3 &= x_2 - x_1 \end{aligned} \tag{3}$$

and $2A = |\eta_1 \zeta_2 - \eta_2 \zeta_1|$ is twice the element area. A mesh of linear stress triangles is shown in Figure 2. Unlike the usual form of the finite element method, each node is unique to a particular element and more than one node may share the same co-ordinates. Statically admissible stress discontinuities are permitted at shared edges between adjacent triangles. If E denotes the number of triangles in the mesh, then there are $3E$ nodes and $9E$ unknown stresses.

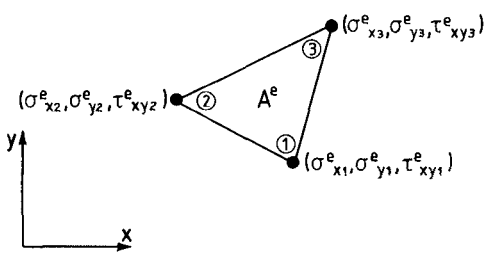

Figure 1. 3-Noded linear stress triangle

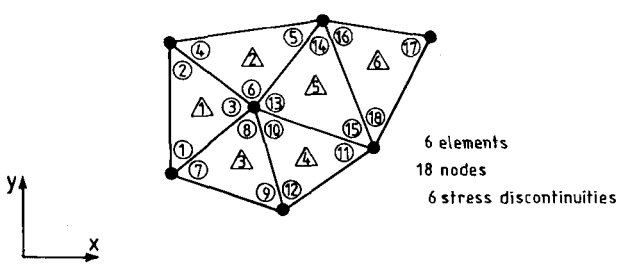

Figure 2. Mesh of linear stress triangles for limit load analysis

Element equilibrium

In order to satisfy equilibrium, the stresses throughout each triangular element must obey the equations

$$\frac{\partial \sigma_x}{\partial x}+\frac{\partial \tau_{xy}}{\partial y}=0; \quad \frac{\partial \sigma_y}{\partial y}+\frac{\partial \tau_{xy}}{\partial x}=\gamma \tag{4}$$

where tensile stresses are taken as positive, γ is the soil unit weight and a right-handed cartesian co-ordinate system is adopted. Using equations (1), (2) and (3) and substituting into the above equation we obtain the equilibrium constraints on the nodal stresses as

$$[A^e_{\text{equil}}]\{\sigma^e\}=\{b^e_{\text{equil}}\} \tag{5}$$

where

$$[A^e_{\text{equil}}]=\frac{1}{2A^e}\begin{bmatrix}\eta_1 & 0 & \zeta_1 & \eta_2 & 0 & \zeta_2 & \eta_3 & 0 & \zeta_3\\ 0 & \zeta_1 & \eta_1 & 0 & \zeta_2 & \eta_2 & 0 & \zeta_3 & \eta_3\end{bmatrix}$$

$$\{\sigma^e\}^{\mathrm{T}}=\{\sigma^e_{x1}\ \sigma^e_{y1}\ \tau^e_{xy1}\ \sigma^e_{x2}\ \sigma^e_{y2}\ \tau^e_{xy2}\ \sigma^e_{x3}\ \sigma^e_{y3}\ \tau^e_{xy3}\} \tag{6}$$

$$\{b^e_{\text{equil}}\}^{\mathrm{T}}=\{0 \quad \gamma^e\}; \quad A^e=\text{area of element}$$

Thus, the equilibrium condition for each triangular element generates two equality constraints on the nodal stresses.

Discontinuity equilibrium

In order to permit statically admissible discontinuities at the edges of adjacent triangles, it is necessary to enforce additional constraints on the nodal stresses. A statically admissible discontinuity permits the tangential stress to be discontinuous, but requires that continuity of the corresponding shear and normal components is preserved. With reference to Figure 3, the normal and shear stresses acting on a plane inclined at an angle θ to the x-axis (measured positive anticlockwise) are given by

$$\begin{aligned}\sigma_n&=\sin^2\theta\,\sigma_x+\cos^2\theta\,\sigma_y-\sin 2\theta\,\tau_{xy}\\ \tau&=-\tfrac{1}{2}\sin 2\theta\,\sigma_x+\tfrac{1}{2}\sin 2\theta\,\sigma_y+\cos 2\theta\,\tau_{xy}\end{aligned} \tag{7}$$

Figure 4 illustrates two triangles, a and b, which share a side d defined by the nodal pairs (1, 2) and (3, 4). Equilibrium of the discontinuity requires that at every point along d

$$\sigma^a_n=\sigma^b_n; \quad \tau^a=\tau^b$$

Since the stresses vary linearly along each element edge, this condition is equivalent to enforcing the constraints

$$\sigma^a_{n1}=\sigma^b_{n2}; \quad \sigma^a_{n3}=\sigma^b_{n4}; \quad \tau^a_1=\tau^b_2; \quad \tau^a_3=\tau^b_4$$

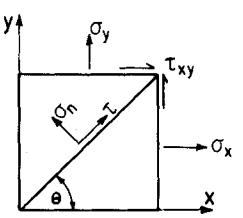

Figure 3. Resolution of stresses into normal and shear components acting on a plane

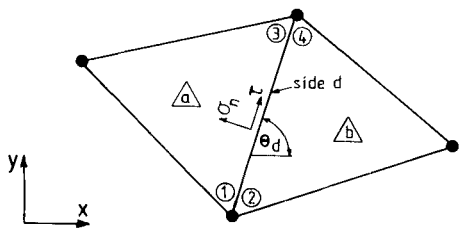

Figure 4. Statically admissible stress discontinuity between adjacent triangles

Substituting equation (7), these equations are summarized by the matrix equation

$$[A^d_{\text{equil}}]\ \{\sigma^d\} = \{b^d_{\text{equil}}\} \tag{8}$$

where

$$[A^d_{\text{equil}}] = \begin{bmatrix} T & -T & 0 & 0 \\ 0 & 0 & T & -T \end{bmatrix}$$

$$[T] = \begin{bmatrix} \sin^2\theta_d & \cos^2\theta_d & -\sin 2\theta_d \\ -\tfrac{1}{2}\sin 2\theta_d & \tfrac{1}{2}\sin 2\theta_d & \cos 2\theta_d \end{bmatrix}$$

$$\{\sigma^d\}^{\mathrm{T}} = \{\sigma^a_{x1}\ \sigma^a_{y1}\ \tau^a_{xy1}\ \sigma^b_{x2}\ \sigma^b_{y2}\ \tau^b_{xy2}\ \sigma^a_{x3}\ \sigma^a_{y3}\ \tau^a_{xy3}\ \sigma^b_{x4}\ \sigma^b_{y4}\ \tau^b_{xy4}\}$$

$$\{b^d_{\text{equil}}\}^{\mathrm{T}} = \{0\ \ 0\ \ 0\ \ 0\} \tag{9}$$

Hence the equilibrium condition for each statically admissible discontinuity along an element edge generates four equality constraints on the nodal stresses.

Boundary conditions

Many problems in geotechnical engineering generate stress boundary conditions of the form

$$\sigma_n = q = \text{constant}; \quad \tau = t = \text{constant} \tag{10}$$

Since each of the stress components σ_x, σ_y and τ_{xy} vary linearly along the edge of each triangle, it is possible to cater for a slightly more general type of boundary condition of the form (see Figure 5)

$$\sigma^l_n = q_1 + (q_2 - q_1)\,\xi; \quad \tau^l = t_1 + (t_2 - t_1)\,\xi \tag{11}$$

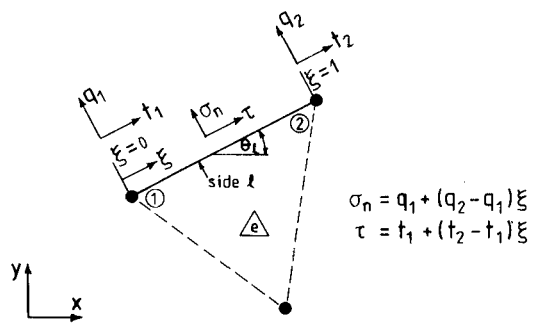

Figure 5. Stress boundary conditions

where

l = edge of triangle e where boundary tractions are specified (defined by nodes 1 and 2)
ξ = local co-ordinate along l
q_1, q_2 = normal stresses specified at nodes 1 and 2 (tension positive)
t_1, t_2 = shear stresses specified at nodes 1 and 2 (clockwise shears around boundary positive)

The boundary conditions defined by (11) are satisfied exactly by requiring that

$$\sigma^e_{n1} = q_1; \quad \sigma^e_{n2} = q_2; \quad \tau^e_1 = t_1; \quad \tau^e_2 = t_2 \tag{12}$$

Letting θ_l denote the angle of l to the axis and using equations (7), the stress boundary conditions give rise to the constraints

$$[A^l_{\text{bound}}]\{\sigma^l\} = \{b^l_{\text{bound}}\} \tag{13}$$

where

$$[A^l] = \begin{bmatrix} T & 0 \\ 0 & T \end{bmatrix}$$

$$[T] = \begin{bmatrix} \sin^2\theta_l & \cos^2\theta_l & -\sin 2\theta_l \\ -\frac{1}{2}\sin 2\theta_l & \frac{1}{2}\sin 2\theta_l & \cos 2\theta_l \end{bmatrix}$$

$$\{\sigma^l\}^{\mathrm{T}} = \{\sigma^e_{x1}\ \sigma^e_{y1}\ \tau^e_{xy1}\ \sigma^e_{x2}\ \sigma^e_{y2}\ \tau^e_{xy2}\} \tag{14}$$

$$\{b^l_{\text{bound}}\}^{\mathrm{T}} = \{q_1\, t_1\, q_2\, t_2\}$$

Thus each edge l, where boundary tractions are prescribed, generates a maximum of four equality constraints on the nodal stresses.

Yield condition

Assuming tensile stresses are taken as positive and plane strain conditions, the Mohr–Coulomb yield criterion may be expressed as

$$F = (\sigma_x - \sigma_y)^2 + (2\tau_{xy})^2 - (2c \cdot \cos\phi - (\sigma_x + \sigma_y)\sin\phi)^2 = 0 \tag{15}$$

In order that the stresses do not violate the yield condition, and hence fulfil the requirements of the lower bound theorem, it is necessary that $F \leq 0$ throughout each triangle. Since we wish to formulate the lower bound theorem as a linear programming problem, it is necessary to approximate (15) by a yield criterion which is a linear function of the unknown stresses. To ensure that the solution obtained is a strict lower bound on the exact collapse load, the linearized yield surface must lie inside the Mohr–Coulomb yield surface in stress space.

Letting

$$X = \sigma_x - \sigma_y; \quad Y = 2\tau_{xy}; \quad R = 2c \cdot \cos\phi - (\sigma_x + \sigma_y)\sin\phi \tag{16}$$

the Mohr–Coulomb yield condition may be written as $X^2 + Y^2 = R^2$. In terms of the variables X and Y, this plots as a circle as shown in Figure 6. The Mohr–Coulomb yield surface is approximated by an interior polygon with p sides and p vertices. The X- and Y- co-ordinates of the kth and $(k+1)$th vertices are given by

$$\begin{aligned} X_k &= R\cos(\pi(2k-1)/p); & Y_k &= R\sin(\pi(2k-1)/p) \\ X_{k+1} &= R\cos(\pi(2k+1)/p); & Y_{k+1} &= R\sin(\pi(2k+1)/p) \end{aligned} \tag{17}$$

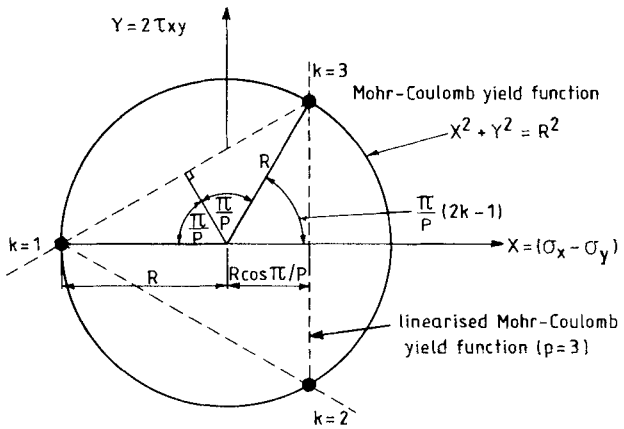

Figure 6. Linearized Mohr–Coulomb yield function ($p=3$)

Each stress point, with co-ordinates X and Y, is located inside or on the yield polygon if

$$(X_{k+1}-X)(Y_k-Y)-(X_k-X)(Y_{k+1}-Y)\leq 0; \quad k=1,2,\ldots,p$$

Substituting equations (16) and (17) gives the linearized yield function as

$$A_k\sigma_x+B_k\sigma_y+C_k\tau_{xy}\leq D; \quad k=1,2,\ldots,p \tag{18}$$

where

$$\begin{aligned} &A_k=\cos(2\pi k/p)+\sin\phi\cos(\pi/p); \quad B_k=\sin\phi\cos(\pi/p)-\cos(2\pi k/p)\\ &C_k=2\sin(2\pi k/p); \qquad\qquad D=2c\cos\phi\cos(\pi/p) \end{aligned} \tag{19}$$

In order that equation (18) is satisfied throughout the mesh it is sufficient to enforce this constraint at each nodal point of each triangle. Moreover, it is not necessary for the cohesion to be constant throughout each triangle. To prove this, let the cohesion vary linearly throughout each triangle according to

$$c=\sum_{i=1}^{3} N_i c_i$$

where N_i are the linear shape functions given by equation (2), and c_i is the cohesion at node i.

The constant D in equation (19) is then a linear function of x and y according to

$$D=\sum_{i=1}^{3} N_i D_i \tag{20}$$

where $D_i=2c_i\cos\phi\cos(\pi/p)$ at node i. Substituting equations (1) and (20) into equation (18) gives the required constraints on the nodal stresses for each triangle as

$$\sum_{i=1}^{3} N_i(A_k\sigma_{xi}+B_k\sigma_{yi}+C_k\tau_{xyi})\leq \sum_{i=1}^{3} N_i D_i; \quad k=1,2,\ldots,p \tag{21}$$

Equation (21) is satisfied throughout a triangle if we enforce the following constraint at each of its nodes:

$$A_k\sigma_{xi}+B_k\sigma_{yi}+C_k\tau_{xyi}\leq D_i; \quad k=1,2,\ldots,p; \quad i=1,2,3 \tag{22}$$

To prove this we note that, by definition, $0 \leqslant N_i \leqslant 1$ for any point inside a triangle and thus

$$N_i(A_k\sigma_{xi}+B_k\sigma_{yi}+C_k\tau_{xyi}) \leqslant N_i D_i;\ k=1,2,\ldots,p;\ i=1,2,3$$

It follows that

$$\sum_{i=1}^{3} N_i(A_k\sigma_{xi}+B_k\sigma_{yi}+C_k\tau_{xyi}) \leqslant \sum_{i=1}^{3} N_i D_i;\ k=1,2,\ldots,p$$

as required. The special case of a purely cohesive soil obeying the linearized Tresca yield criterion is obtained by setting $\phi=0$ in equations (19). Since the cohesion is permitted to vary linearly throughout each triangle, a purely cohesive soil which has cohesion increasing linearly with depth can also be dealt with.

The constraints imposed on the stresses at node i due to the linearized yield criterion may be summarized by the matrix equation

$$[A^i_{\text{yield}}]\{\sigma^i\} \leqslant \{b^i_{\text{yield}}\} \tag{23}$$

where

$$[A^i_{\text{yield}}] = \begin{bmatrix} A_1 & B_1 & C_1 \\ A_2 & B_2 & C_2 \\ \cdot\cdot & \cdot\cdot & \cdot\cdot \\ A_k & B_k & C_k \\ \cdot\cdot & \cdot\cdot & \cdot\cdot \\ A_p & B_p & C_p \end{bmatrix}$$

$$\{\sigma^i\}^{\mathrm{T}} = \{\sigma_{xi}\sigma_{yi}\tau_{xyi}\} \tag{24}$$

$$\{b^i_{\text{yield}}\}^{\mathrm{T}} = \{2c_i\cos\phi\cos(\pi/p)\ \ 2c_i\cos\phi\cos(\pi/p), \ldots, 2c_i\cos\phi\cos(\pi/p)\}$$

The coefficients A_k, B_k, C_k are given by equations (19) and c_i is the cohesion at node i. Hence the linearized yield condition generates p inequality constraints on each nodal stress vector. Since there are $3E$ nodes for a mesh of E triangles, the total number of inequality constraints generated is $3pE$.

Objective function

For most plane strain geotechnical problems, we wish to find a statically admissible stress field which maximises an integral of the form

$$Q = h\int_s \sigma_n \mathrm{d}s$$

where Q is the collapse load, h is the out-of-plane thickness, and σ_n is the normal stress acting over some part of the boundary s. Figure 7 illustrates an edge of a triangle, defined by nodes 1 and 2, over which σ_n is to be maximized. Since the stresses are assumed to vary linearly throughout each element, Q is given by

$$Q = \frac{Lh}{2}(\sigma_{n1}+\sigma_{n2}) \tag{25}$$

where L is the length of the edge s and σ_{n1}, σ_{n2} are the normal stresses at nodes 1 and 2 of triangle e. Letting θ_s denote the inclination of s to the x-axis, assuming unit thickness in the out-of-plane

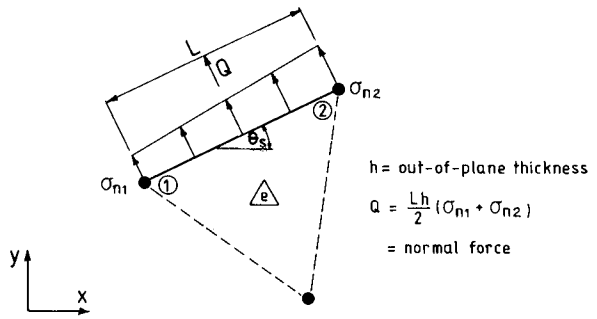

Figure 7. Load in a direction normal to a boundary edge

direction, and substituting equation (7) we obtain

$$Q=\{c^s\}^{\mathrm{T}}\{\sigma^s\} \tag{26}$$

where

$$\{c^s\}^{\mathrm{T}}=\frac{L}{2}\{\sin^2\theta_s\cos^2\theta_s-\sin2\theta_s\sin^2\theta_s\cos^2\theta_s-\sin2\theta_s\}$$

$$\{\sigma^s\}^{\mathrm{T}}=\{\sigma^e_{x1}\ \sigma^e_{y1}\ \tau^e_{xy1}\ \sigma^e_{x2}\ \sigma^e_{y2}\ \tau^e_{xy2}\} \tag{27}$$

In linear programming terminology, $\{c^s\}$ is known as the vector of objective function coefficients and has units of area. Since it has been assumed that σ_n is positive for tensile loading, it is necessary to multiply $\{c^s\}$ by -1 if a compressive load is to be maximized.

Assembly of constraint equations

All of the steps that are necessary to formulate the lower bound theorem as a classical linear programming problem have now been covered. The only step remaining is to assemble the constraint matrices and objective function coefficients for the overall mesh.

Using equations (5), (8), (13) and (23), the various constraints may be assembled to give the overall constraint matrix according to

$$[A]=\sum_{i=1}^{N}[A^i_{\text{yield}}]+\sum_{e=1}^{E}[A^e_{\text{equil}}]+\sum_{d=1}^{D}[A^d_{\text{equil}}]+\sum_{l=1}^{L}[A^l_{\text{bound}}]$$

where the coefficients are inserted into the appropriate rows and columns and N is the total number of nodes, E is the total number of elements, D is the total number of discontinuities and L is the total number of boundary edges with prescribed tractions.

Similarly, the vector $\{b\}$ and objective function coefficients $\{c\}$ are assembled according to

$$\{b\}=\sum_{i=1}^{N}\{b^i_{\text{yield}}\}+\sum_{e=1}^{E}\{b^e_{\text{equil}}\}+\sum_{d=1}^{D}\{b^d_{\text{equil}}\}+\sum_{l=1}^{L}\{b^l_{\text{bound}}\}$$

$$\{c\}=\sum_{s=1}^{S}\{c^s\}$$

where S is the total number of boundary edges over which the normal stresses are to be optimized.

The problem of finding a statically admissible stress field which maximizes the collapse load may thus be stated

Maximize $\{c\}^T\{\sigma\}$
Subject to $[A]\{\sigma\} \leqslant \{b\}$

where $\{\boldsymbol{\sigma}\}$ is a vector of nodal stresses given by

$$\{\sigma\}^T = \{\sigma_{x1}\ \sigma_{y1}\ \tau_{xy1} \quad \sigma_{x2}\ \sigma_{x2}\ \tau_{xy2} \ \ldots\ \sigma_{xN}\ \sigma_{yN}\ \tau_{xyN}\}$$

This may also be written in the form

$$\begin{aligned} &\text{Minimize} && -\{c\}^T\{\sigma\} \\ &\text{Subject to} && [A_1]\{\sigma\} \leqslant \{b_1\} \\ & && [A_2]\{\sigma\} = \{b_2\} \end{aligned} \tag{28}$$

where $[A_1]$ is the matrix of yield constraints and $[A_2]$ is a matrix of all the other equality constraints. Various strategies for solving this linear programming problem are discussed in the next section.

SOLUTION PROCEDURE

Before discussing various strategies for solving the resulting linear programming problem, it is instructive to examine the nature of the constraint matrix $[A]$. The characteristics of this matrix have an important bearing on the choice of solution algorithm.

Assuming that stress discontinuities are permitted to occur at all edges shared by adjacent triangles, there will be $3E$ nodes for a mesh of E triangles. Since each node is associated with 3 stresses, the total number of unknowns, n, is $9E$. The total number of rows in the constraint matrix is

$$m = m_y + m_t + m_d + m_b$$

where

m_y = the number of yield inequalities $= 3pE$
m_t = the number of triangle equilibrium equalities $= 2E$
m_d = the number of discontinuity equilibrium equalities $= 4(E + N_c - 1 - B)$
m_b = the number of boundary condition equalities $= 4B$

In the above, N_c is the number of unique nodal co-ordinates and B is the number of boundary edges. Note that the total number of edges in a triangulation is given by Euler's theorem for planar graphs and is equal to $E + N_c - 1$. Thus the number of discontinuities is given by $E + N_c - 1 - B$ and the maximum number of nonzero coefficients is equal to $3m_y + 6m_t + 6m_d + 3m_b$. If we define the density of the constraint matrix as

$$\rho = \frac{\text{number of nonzero coefficients}}{\text{number of rows} \times \text{number of columns}}$$

it follows that

$$\rho = \frac{3pE + 12E + 8N_c - 4B - 8}{3E(3pE + 6E + 4N_c - 4)}$$

For a reasonably fine mesh, it may be shown that $N_c \simeq \frac{1}{2}E$ and hence

$$\rho \simeq \frac{3p + 16}{3E(3p + 8)}$$

For typical values of p and E, the constraint matrix is thus extremely sparse. Choosing $p=12$ and $E=50$, for example, the density is approximately 2 per cent. In practical applications it has been found that the density is often less than 1 per cent. Another feature of the constraint matrix, which is especially important for linear programming applications, is that there are usually many more rows than columns. Indeed it is readily shown that for a relatively fine mesh

$$\frac{m}{n} \simeq \frac{3p+8}{9}$$

For values of p of about 12, this implies that there will be roughly 5 times as many rows in the constraint matrix as there are columns. Moreover, this ratio will increase with increasing p.

The revised simplex and active set algorithms

A comprehensive discussion of the theory and implementation of the revised simplex and active set algorithms may be found in Best and Ritter.[7] Since a formal statement of these techniques is beyond the scope of this paper, only their salient features will be noted.

Before applying the revised simplex algorithm, it is usually necessary to express the problem in the following canonical form:

$$\begin{aligned} &\text{Minimize} && \{c^*\}^{\mathrm{T}}\{x^*\} \\ &\text{Subject to} && [A^*]\{x^*\}=\{b^*\} \\ & && \{x^*\}\geqslant\{0\} \end{aligned} \tag{29}$$

Equation (28) may be converted to the above form by defining

$$\{c^*\}^{\mathrm{T}}=\{-\{c\}^{\mathrm{T}} \quad \{c\}^{\mathrm{T}} \quad \{0\}^{\mathrm{T}}\}$$

$$\{x^*\}^{\mathrm{T}}=\{\{\sigma^+\}^{\mathrm{T}} \quad \{\sigma^-\}^{\mathrm{T}} \quad \{s\}^{\mathrm{T}}\}$$

$$\{b^*\}^{\mathrm{T}}=\{\{b_1\}^{\mathrm{T}} \quad \{b_2\}^{\mathrm{T}}\}$$

$$[A^*]=\begin{bmatrix} [A_1] & -[A_1] & [\mathrm{I}] \\ [A_2] & -[A_2] & [0] \end{bmatrix}$$

where

$$\{\sigma\}=\{\sigma^+\}-\{\sigma^-\}$$

$$\{\sigma^+\},\ \{\sigma^-\},\ \{s\}\geqslant\{0\}$$

In the above, $\{s\}$ is a vector of slack variables that are added to the yield inequalities and $[I]$ is the identity matrix. The vectors $\{\sigma^+\}$ and $\{\sigma^-\}$ arise because the stresses are unrestricted in sign. In the solution of (29), the revised simplex algorithm works with a basis matrix which is of dimension $m \times m$. Each iteration updates this matrix and requires $0(m^2)$ operations. Thus the revised simplex algorithm is most suited to problems where $m<n$. Since the formulation of the lower bound theorem gives rise to constraint matrices which may have a very large number of rows, it is apparent that the revised simplex algorithm should not be applied directly to equation (28). The performance of the technique can be improved considerably by solving the dual of (28). In linear programming terminology, (28) is known as the primal problem. It may be shown[7] that the corresponding dual linear programming problem is

$$\begin{aligned} &\text{Minimize} && \{b_1\}^{\mathrm{T}}\{u_1\}+\{b_2\}^{\mathrm{T}}\{u_2\} \\ &\text{Subject to} && [A_1]^{\mathrm{T}}\{u_1\}+[A_2]^{\mathrm{T}}\{u_2\}=\{c\};\quad \{u_1\}\geqslant\{0\} \end{aligned}$$

This may be written in the canonical form required by the revised simplex method by defining

$$\{c^*\}^T = \{\{b_1\}^T \{b_2\}^T - \{b_2\}^T\}$$
$$\{x^*\}^T = \{\{u_1\}^T \{u_2^+\}^T \{u_2^-\}^T\}$$
$$\{b^*\} = \{c\}$$
$$[A^*] = [[A_1]^T [A_2]^T - [A_2]^T]$$

where

$$\{u_2\} = \{u_2^+\} - \{u_2^-\}; \quad \{u_1\}, \{u_2^+\}, \{u_2^-\} \geqslant \{0\}$$

The advantage of solving the dual problem by the revised simplex method is that the overall constraint matrix now has many more columns than rows. Moreover the number of rows is substantially less than that of the corresponding primal problem. Once the dual solution has been obtained, it is a trivial process to obtain the solution of the primal problem (see Reference 7 for a comprehensive discussion on duality theory and the extraction of dual solutions).

Although the lower bound linear programming problem can be solved in a reasonably efficient manner by using duality theory and the revised simplex method, an even more elegant and efficient approach is to employ the active set algorithm developed by Best and Ritter.[7] The canonical form required by this technique is

Minimize $\{c^*\}^T\{x^*\}$

Subject to $[A_1^*]\{x^*\} \leqslant \{b_1^*\}$

$[A_2^*]\{x^*\} = \{b_2^*\}$

Equation (28) may be written in this form simply by defining

$$\{c^*\} = -\{c\}; \quad \{x^*\} = \{\sigma\}$$
$$\{b_1^*\} = \{b_1\}; \quad \{b_2^*\} = \{b_2\}$$
$$[A_1^*] = [A_1]; \quad [A_2^*] = [A_2]$$

The canonical form required by the active set strategy thus follows naturally from the formulation of the lower bound linear programming problem.

The active set algorithm works with the inverse of the active constraint matrix, which is of dimension $n \times n$. This matrix is updated at each iteration which requires $O(n^2)$ operations. Thus this algorithm is ideally suited to the lower bound linear programming problem where the overall constraint matrix has many more rows than columns.

Implementation of the active set strategy

A FORTRAN-77 implementation of the active set strategy may be found in Best and Ritter.[7] A number of modifications to this code have been made by the author to improve efficiency and reduce the storage requirements. The most important modifications are:

1. Only the nonzero entries in the constraint matrix are stored. For the active set algorithm it is convenient to store the entries row by row.
2. The active constraint matrix is factorized and updated using the routines given by Reid.[12] These codes fully exploit the extreme sparsity of the constraint matrix and have been found to be very stable and efficient.

The active set algorithm, when combined with the sparse factorization routines of Reid, is a very

efficient method for solving the lower bound linear programming problem (both in terms of storage and CPU time). Because of the relatively modest memory demands, very large problems may be solved in-core. All of the analyses presented in this paper were run on a VAX 8550 at The University of Newcastle using double precision arithmetic.

APPLICATIONS

To illustrate the effectiveness of the procedure described previously, a number of footing examples are analysed and the results compared with known exact solutions. Both purely cohesive (including increasing strength with depth) and cohesive-frictional soil models are assumed.

Undrained loading of smooth strip footings

The well-known Prandtl solution for this problem gives the exact collapse pressure as $q_f = N_c c_u$, where c_u is the undrained shear strength and $N_c = 2 + \pi$. The meshes used to analyse this problem are shown in Figure 8 and the results are summarized in Table I for various values of p (the number

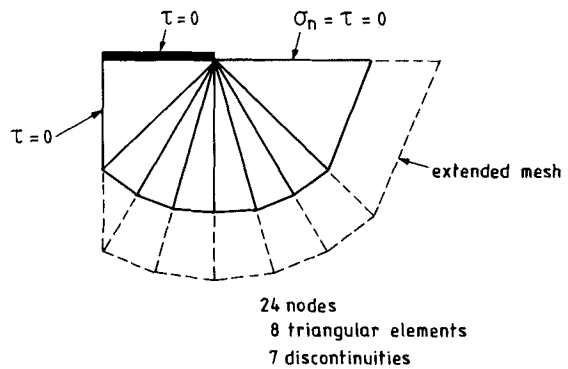

Figure 8. Meshes for smooth strip footing on purely cohesive soil ($\phi_u = 0$)

Table I. Results for smooth rigid footing on a purely cohesive soil ($\phi_u = 0$)

p	n	m	i	t	N_c
6	72	195	40	0·5	4·72
12	72	339	58	0·7	5·03
24	72	627	85	1·4	5·06
48	72	1203	125	2·9	5·07
48†	72	1203	210	4·2	5·08

Notes:
p = number of sides in linearized polygon;
n = number of rows in constraint matrix;
m = number of rows in constraint matrix;
i = total number of iterations for active set algorithm;
t = CPU time (sec) for VAX 8550 operating under VMS with the optimizing FORTRAN-77 compiler.
† Results for extended mesh.

of sides in the linearized yield polygon). For p values of 24 and 48, the lower bound estimate of the collapse load is within 1 per cent of the exact solution. Generally speaking, it has been found that choosing p greater than 12 gives a sufficiently accurate approximation to the Tresca yield function for undrained loading conditions. Note that the CPU time requirement is approximately proportional to p. This is in contrast to the findings of Lysmer[1] who, using the traditional simplex algorithm, found that the CPU time grew at a rate roughly proportional to p^3. In order to verify that the solutions presented in Table I are valid for an infinite half-space, it is necessary to show that the lower bound stress field can be extended downwards and to the right without affecting the collapse load. The extended mesh shown in Figure 8 yielded values for N_c which are almost identical to those obtained for the smaller mesh. Thus it is reasonable to assume that the results presented in Table I are true lower bounds for the case of an infinite half-space.

Drained loading of smooth strip footings

The exact collapse pressure for a smooth strip footing resting on a cohesive-frictional soil may be written as

$$q_f = N_c c' + qN_q$$

where

$$N_q = \exp(\pi \tan\phi') \tan^2(\pi/4 + \phi'/2); \quad N_c = (N_q - 1)\cot\phi'$$

and q is the overburden pressure. For the case of a surface footing we have

$$N_q = \frac{q_f}{c'\cot\phi'} + 1$$

The meshes used to analyse this problem are shown in Figure 9. For $c' = 1$ and $\phi' = 40°$ the exact value for N_q is 64·20. This value may be compared with the numerical lower bounds given in Table II. Due to the dependence of the Mohr–Coulomb yield function on hydrostatic pressure, we see that the lower bound solution is much more sensitive to the number of sides used in the linearized yield polygon. At least 24 sides are necessary to model the parent yield function with sufficient accuracy. For values of p equal to 24 and 48, the lower bound analysis estimates the exact collapse load to within 7·0 per cent and 4·4 per cent respectively. As with the undrained case, the CPU time grows at a rate which is roughly proportional to p. Analysis with the extended mesh shown in Figure 9 yielded values for N_q which are almost identical to those for the smaller mesh. Thus it is

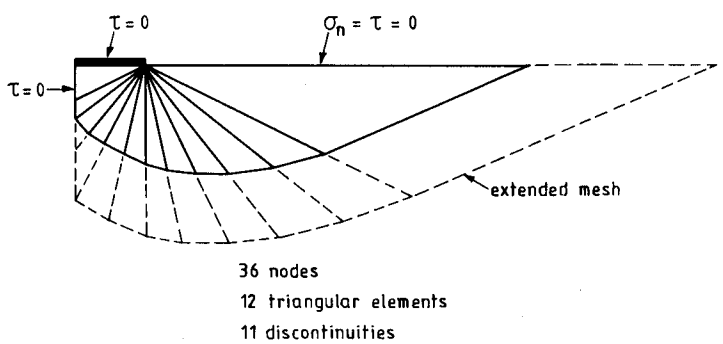

Figure 9. Meshes for smooth strip footing on cohesive-frictional soil ($c' = 1$, $\phi' = 40°$)

Table II. Results for smooth rigid footing on a cohesive-frictional soil ($c'=1$, $\phi'=40°$)

p	n	m	i	t	N_q
6	108	293	112	1·6	35·68
12	108	509	156	2·6	53·58
24	108	941	219	4·6	59·69
48	108	1805	421	12·5	61·35
48†	108	1805	404	11·4	61·11

† Results for extended mesh.

reasonable to assume that the solutions presented in Table II are valid for the case of an infinite half-space.

Undrained loading of strip footing (strength increasing with depth)

The exact collapse pressure for a rigid strip footing resting on a purely cohesive soil, where strength increases linearly with depth, has been derived by Davis and Booker.[9] Their solutions may be written in the form

$$q_f = F[(2+\pi)c_{uo} + \rho B/4]$$

In this equation, c_{uo} is the undrained shear strength at the soil surface, $\rho = dc_u/dz$, where z is the depth measured from the soil surface and B is the footing width. The factor F is a function of the dimensionless quantity $\rho B/c_{uo}$ and is different for smooth and rough footings. Choosing $\rho B/c_{uo}=3$ and $c_{uo}=1$ the above equation gives $F=q_f/5{\cdot}89$. Using the charts provided in Davis and Booker,[9] the exact value of F for a smooth rigid footing with the above parameters is $F_s \simeq 1{\cdot}22$. The meshes used to analyse this problem are shown in Figure 10. For a p value of 24, the lower bound analysis gives $F_s = 1{\cdot}20$ and thus underestimates the exact value by approximately 1·6 per cent.

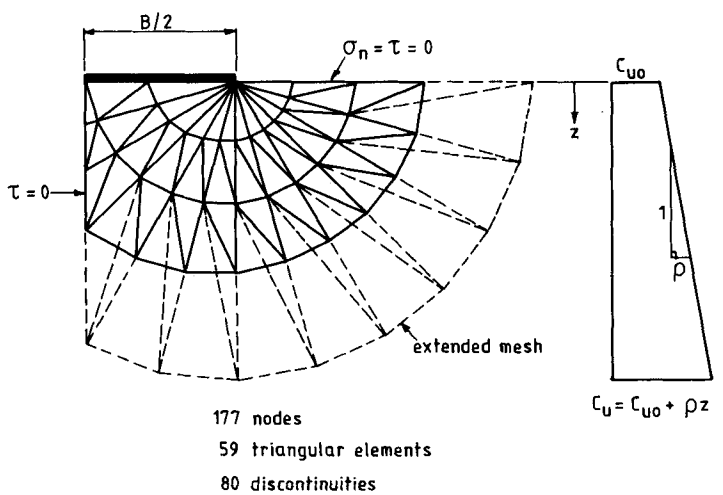

Figure 10. Meshes for rigid strip footing on purely cohesive soil ($\phi_u=0$, increasing strength with depth, $\rho B/c_{uo}=3$, $c_{uo}=1$)

Analysis with the extended mesh shown in Figure 10 yielded an identical value for F_s and thus it may be concluded that the results from the lower bound calculations are applicable to a footing resting on an infinite half-space. In the case of a rough rigid footing, the exact value for F is approximately 1·42. Analysis with both of the meshes shown in Figure 10 gives $F_r = 1{\cdot}36$ which underestimates the true collapse load by 4·2 per cent.

The linear programming formulation for the above problems leads to a constraint matrix with 531 columns and 4707 constraints (4703 constraints for the rough footing). On the VAX 8550 at The University of Newcastle, the CPU time required was approximately 2 minutes. In the author's experience, this is substantially less than the CPU time required for a high quality finite element analysis. The lower bound analysis, of course, has the distinct advantage that it provides a strict lower bound on the true collapse load, whereas the displacement type of finite element formulation provides a solution which is neither a strict upper bound nor a strict lower bound.

CONCLUSIONS

A method for computing rigorous lower bounds on the collapse load for plane problems in soil mechanics has been described. The technique uses finite elements and linear programming to compute statically admissible stress fields. Since these stress fields satisfy all of the requirements of the lower bound theorem of classical plasticity theory, the resulting solutions are strict lower bounds on the true collapse loads and therefore 'safe'. It is expected that the main application of the technique will be to produce stability charts for various problems in soil mechanics that are unsuitable for solution by conventional methods. Major advantages of the procedure include the ability to deal with complicated loadings, complex geometries and inhomogeneous soil properties. Due to the efficiency of the sparse active set algorithm, the method is appreciably faster than the displacement type of finite element method for predicting collapse loads.

ACKNOWLEDGEMENTS

The author would like to thank Professor J. R. Booker for stimulating discussions on the finer points of classical plasticity theory and Miss Cherie Hook for her typing of the manuscript.

REFERENCES

1. J. Lysmer, 'Limit analysis of plane problems in soil mechanics', *J. Soil Mech. Found. Div., A.S.C.E.*, **96** (SM4), 1311–1334 (1970).
2. E. H. Davis, 'Theories of plasticity and the failure of soil masses', in *Soil Mechanics—Selected Topics* (Ed. I. K. Lee), Chap. 6, Butterworths, London, 1968.
3. W. F. Chen, *Limit Analysis and Soil Plasticity*, Elsevier, Amsterdam, 1975.
4. E. Anderheggen and H. Knopfel, 'Finite element limit analysis using linear programming', *Int. J. Solids Struct.*, **8**, 1413–1431 (1972).
5. J. Pastor, 'Application de l'analyse Limite a l'etude de la Stabilitie des Pentes et des Talus', *Thesis*, Institute of Mechanics, Grenoble (1976).
6. A. Bottero, R. Negre, J. Pastor and S. Turgeman, 'Finite element method and limit analysis theory for soil mechanics problems', *Comp. Meth. Appl. Mech. Eng.*, **22**, 131–149 (1980).
7. M. J. Best and K. Ritter, *Linear Programming: Active Set Analysis and Computer Programs*, Prentice-Hall, New Jersey, 1985.
8. P. E. Gill, W. Murray and M. H. Wright, *Practical Optimisation*, Academic Press, London, 1981.

9. E. H. Davis and J. R. Booker, 'The effect of increasing strength with depth on the bearing capacity of clays', *Geotechnique*, **23** (4), 551–563 (1973).
10. P. K. Basudhar, A. J. Valsangkar and M. R. Madhar, 'Optimal lower bound of passive earth pressure using finite elements and nonlinear programming', *Int. j. numer. anal. methods geomech.*, **3**, 367–379 (1979).
11. R. Casciaro and L. Cascini, 'A mixed formulation and mixed finite elements for limit analysis', *Int. j. numer. methods eng.*, **18**, 211–243 (1982).
12. J. K. Reid, 'FORTRAN subroutines for handling sparse linear programming bases', *Harwell Report*, A.E.R.E., R8269 (1976).